Short communication

Dynamic-temperature operation of metal-supported solid oxide fuel cells
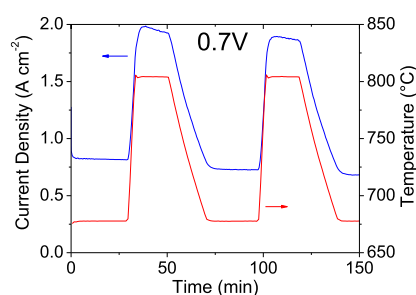
Michael C. Tucker*

Energy Conversion Group, Energy Technologies Area, Lawrence Berkeley National Laboratory, 1 Cyclotron Rd, Berkeley, CA, 94720, USA

HIGHLIGHTS

- Dynamic-temperature operation proposed as new SOFC operation mode.
- Metal-supported SOFCs are operated continuously while temperature is cycled.
- Current doubles in a few minutes by rapidly increasing temperature.

GRAPHICAL ABSTRACT

ABSTRACT

A dynamic-temperature operation strategy is proposed for SOFC systems, in which the cell temperature varies rapidly to match the SOFC stack power output to a dynamic load requirement. It is anticipated that this operation strategy may have benefits for system efficiency, size, and cost for applications with dynamic power load. Metal-supported SOFCs (MS-SOFCs) are operated continuously at 0.7 V while the temperature is varied rapidly between 675 and 800 °C or 670 and 720 °C. During the initial thermal excursion, the current density increases from 0.82 to 1.95 A cm^{-2} in 6.6 min for 675–800 °C, and from 1.0 to 1.63 A cm^{-2} in 5.4 min for 670–720 °C. Cells are subjected to continuous dynamic temperature operation for more than 100 cycles.

1. Introduction

Solid oxide fuel cells (SOFCs) operate at elevated temperature in the range 600–900 °C. Conventional anode-supported cells (ASCs) are typically operated near isothermally and with slow start-up and shutdown temperature ramp rates to avoid brittle failure of the cells arising from inhomogeneous thermal expansion stress. Power output from an SOFC is dictated by the I-V polarization curve at a given operating temperature, and it is routine to select different voltage/current operating points along the curve when adjusting power output to meet demand. As voltage is decreased, however, efficiency of the system suffers as ohmic, kinetic, and mass transport losses increase. SOFC system demonstrations therefore often operate at base load around 0.7–0.9 V [1–4], providing a good balance between efficient use of the fuel and cell output power density, which is directly related to capital cost of the system. Many potential applications for SOFC power systems, however, display power demands that are constantly fluctuating. The grid experiences large daily and annual variations in power demand, and output from smaller systems for distributed, data center, aerospace, vehicular, or personal power generation can vary on a minute-to-minute basis or faster. We propose dynamic-temperature operation of SOFC systems as a method to more closely match the capabilities of the SOFC to the requirements of the applications. It is envisioned as a control strategy wherein the cell temperature varies rapidly to meet transient load requirements; cell voltage or current variation could be limited while still providing higher temporary peak power at a higher temperature. By introducing temperature as an additional control variable, the system can maintain operation above 0.7 V for high
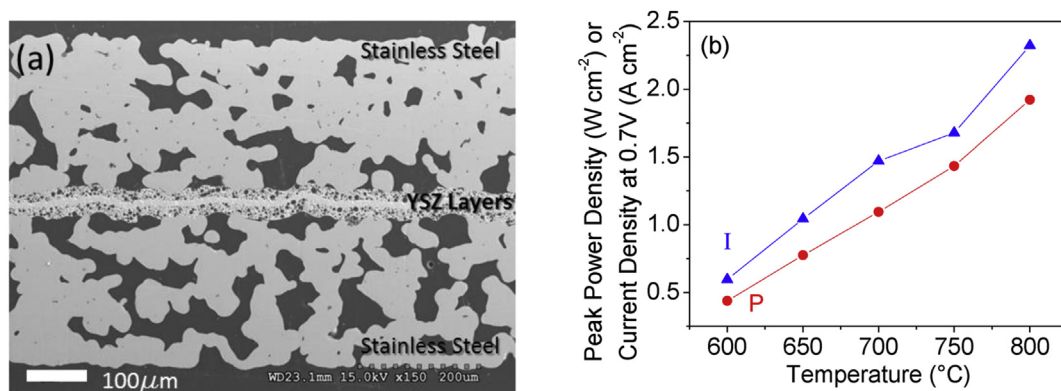
Fig. 1. MS-SOFC (a) architecture and (b) temperature-dependent performance. Current density at 0.7 V (blue triangles) and peak power density (red circles). Image reproduced and data derived from Ref. [11] with the permission of the publisher. (For interpretation of the references to colour in this figure legend, the reader is referred to the Web version of this article.)
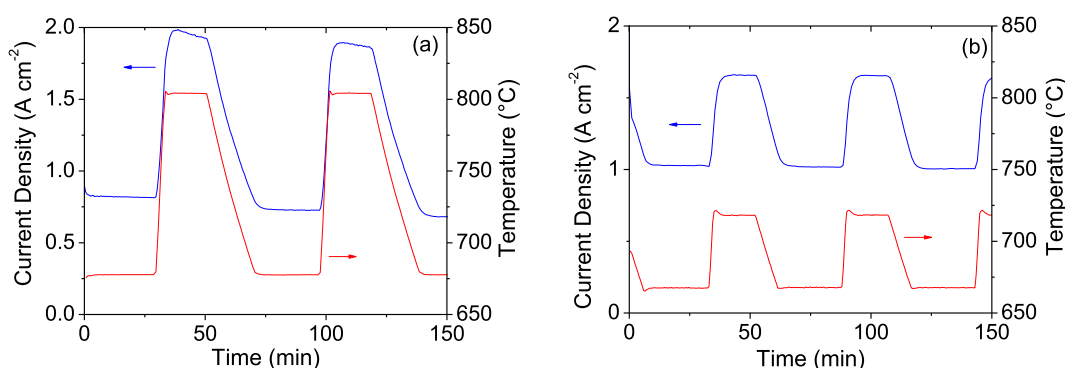

Fig. 2. Dynamic-temperature operation. Potentiostatic operation at 0.7 V while current (upper blue line) is monitored and temperature (lower red line) is varied. Temperature cycling is approximately between (a) 675 and 800 °C or (b) 670 and 720 °C. (For interpretation of the references to colour in this figure legend, the reader is referred to the Web version of this article.)
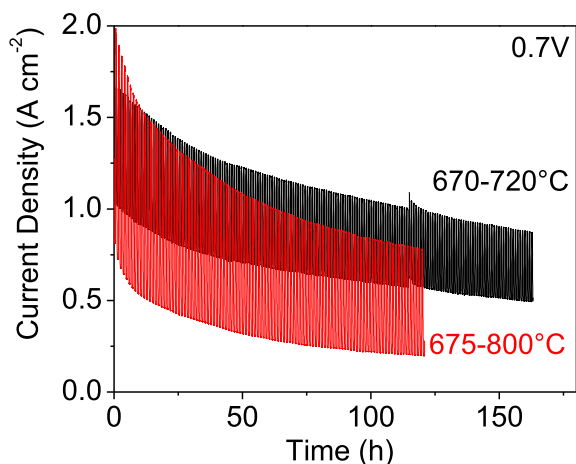

Fig. 3. Long-term dynamic-temperature operation at 0.7 V with temperature cycled between 675 and 800 °C (bottom red line) or 670 and 720 °C (top black line). (For interpretation of the references to colour in this figure legend, the reader is referred to the Web version of this article.)

efficiency, while modulating power output to meet demand. For example, a SOFC system producing baseload power over night could be operated at higher temperature for a few hours during the afternoon to meet peak power requirements. In another scenario, a SOFC propulsion system for an unmanned aerial vehicle (UAV) could operate at high temperature to meet lift-off power demands, then cool down quickly for cruising. It is anticipated that this strategy may also reduce capital cost of SOFC systems, as stack size can be selected for baseload rather than

peak power demand. In other words, a relatively smaller and therefore less costly SOFC stack can meet peak power demand by allowing operating temperature to vary.

Metal-supported SOFCs (MS-SOFCs) are particularly well suited to dynamic-temperature operation due to their tolerance to thermal cycling. Showing that temperature can be considered a control variable, a full MS-SOFC operating stack was simulated to cool approximately 25 °C in 10 min, while voltage, current, and efficiency varied [5]. In contrast to the present work, only a single cooling event with relatively small temperature difference was reported, and the results were simulated rather than being demonstrated on a real system. LBNL previously demonstrated repeated startup of a bare planar MS-SOFC from room temperature to above 700 °C in only 10 s via flame impingement, and 200 cycles for a cell sealed to a test rig with 15 min furnace heatup from 80 to 700 °C [6,7]. MS-SOFCs with a novel composite anode were cycled 100 times with 45 °C min^{-1} heating rate [8]. Tubular MS-SOFCs have been thermal cycled 250 times at 10 °C min^{-1} [9], and 5 times at 350 °C min^{-1} maximum rate [10]. Thermal cycling is typically performed over a temperature range from near room temperature to the operating temperature, with the cell held at open circuit (no power generated) during temperature ramps. This standard protocol is relevant to start-up and shut-down of a system. In contrast, the present work demonstrates continuous operation of the cell during rapid temperature cycles over a wide range of operating temperatures, relevant to the dynamic-temperature operation strategy discussed above.

2. Experimental methods

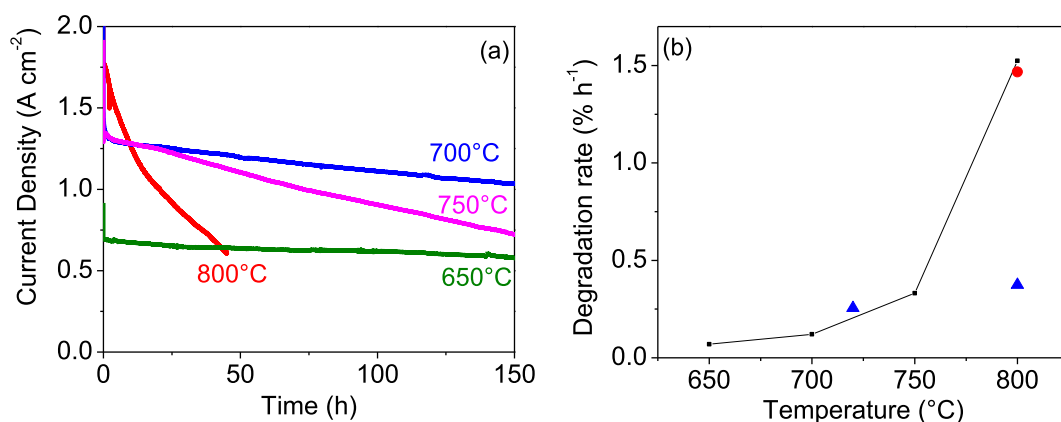Details of the cell fabrication and catalyst infiltration procedures are

Fig. 4. Impact of dynamic-temperature operation on degradation of MS-SOFC. (a) Isothermal operation at 0.7 V. (b) Comparison of degradation rates for isothermal operation (black line) and dynamic-temperature operation at 0.7 V with peak temperature indicated on the abscissa. Degradation rate is calculated using the entire operation time (blue triangles) or cumulative time at 800 °C or above (red circle). (For interpretation of the references to colour in this figure legend, the reader is referred to the Web version of this article.)

discussed elsewhere [11]. MS-SOFCs were fabricated from YSZ (8Y, Tosoh) and stainless steel (P434L alloy, water atomized, Ametek Specialty Metal Products) layers prepared by tape-casting. Individual tapes were laminated together to create the green cell structure. Cells were cut from the layered tape with a laser cutter (H-series, Full Spectrum Laser). Cells were debinded in air at 525 °C for 1 h, and then sintered in 2% hydrgen in argon at 1350 °C for 2 h in a tube furnace. Final cell shape was a circular button cell of 30 mm diameter. After sintering, cells were infiltrated by techniques described previously [12,13] with $La_{0.15}Sr_{0.85}MnO_{3-d}$ (LSM) on the cathode side and $Sm_{0.2}Ce_{0.8}O_{2-d}$ (SDC) mixed with Ni with a ceria:Ni volume ratio of 80:20 on the anode side.

Complete cells were mounted to a 410 stainless steel test rig using GM31107 (Schott) sealing glass, as described previously [7]. Each side of the cell was contacted with two NiCr wires, attached with a small piece of platinum mesh spot-welded to the wire and the cell. Cell performance was assessed with a potentiostat (Biologic SP-150 with 5 A current booster), operated potentiostatically at 0.7 V. Thermal cycling was accomplished by leaving the test rig and cell in a clam-shell tube furnace and adjusting the furnace temperature. Temperature at the cell was recorded with a type K thermocouple and temperature logger (Madgetech Temp101 A).

3. Results and discussion

The MS-SOFC architecture shown in Fig. 1 is symmetric, with porous stainless steel supports and porous YSZ electrode layers bonded to both sides of the YSZ electrolyte. Nano-scale catalysts are introduced into both electrodes by infiltration, as described in recent work [11]. Fig. 1b shows the temperature dependence for peak power density and current density at 0.7 V, both of which vary approximately linearly with temperature. Increasing the operating temperature from 650 °C to 800 °C results in more than a doubling of current density at 0.7 V. With MS-SOFCs easily tolerating heating rate greater than 40 °C min^{-1}, ramping over this temperature range to meet fluctuating power demand could occur in less than 4 min.

The concept of dynamic temperature operation is demonstrated in Fig. 2. This demonstration of tolerance to thermal excursions while under load extends the results of previous work regarding rapid thermal cycling under no load. A MS-SOFC is operated continuously at 0.7 V while the temperature is ramped up and down in the range between approximately 675 and 800 °C (Fig. 2a) or 670 and 720 °C (Fig. 2b). Heating occurs in 4.2 min up to 800 °C or 2.6 min up to 720 °C. Cooling takes somewhat longer due to the furnace insulation. Note that the heating rate is limited by the furnace power, not by the thermal cycling tolerance of the MS-SOFC. The increase in current density lags the

thermocouple temperature slightly, presumably due to the thermal mass of the cell and test rig. During the initial thermal excursion, the current density increases from 0.82 to 1.95 A cm^{-2} in 6.6 min for 675–800 °C, and from 1.0 to 1.63 A cm^{-2} in 5.4 min for 670–720 °C. This is a dramatic and continuous change in the MS-SOFC's power capability in a few minutes, while continuously operating at a fixed voltage setpoint.

Each cell was cycled continuously for more than 120 h, as shown in Fig. 3. The cell with 800 °C peak temperature was cycled 107 times, and the cell with 720 °C peak temperature was cycled 174 times. Degradation for the cell with 800 °C peak operating temperature is clearly more rapid than for 720 °C peak temperature. This is not surprising, as the primary degradation modes for this type of MS-SOFC are catalyst coarsening and Cr deposition in the cathode, both of which are accelerated at higher temperature, and lead to more rapid degradation than typically observed in conventional SOFCs [7]. The large impact of operating temperature on degradation rate is illustrated in Fig. 4. Isothermal operation of MS-SOFCs at 0.7 V is shown in Fig. 4a, and the dramatic acceleration of degradation rate with increased temperature is summarized in Fig. 4b. It is not obvious, however, whether the degradation observed during dynamic temperature cycling (Fig. 3) is dominated by thermal exposure at the higher operating temperatures, or if additional degradation modes arise from the aggressive temperature cycling. To elucidate this, degradation rates for dynamic temperature operation are compared with the isothermal degradation in Fig. 4b. The cell with peak temperature of 720 °C shows similar degradation to that expected from the isothermal data. In contrast, the cell with peak temperature of 800 °C shows much lower degradation. Recognizing that the majority of thermally-activated degradation will occur when the cell is held near 800 °C, a modified degradation rate was calculated based only on cumulative time that the operating temperature was at or above 800 °C (26% of the total time, see Fig. 2a). This agrees quite well with the degradation observed for isothermal operation at 800 °C. These results suggest that degradation during dynamic-temperature operation is dominated by thermal exposure, and that additional significant degradation arising from thermal excursions does not occur. To minimize degradation, the operating temperature can be constrained to a range where long-term stable isothermal operation is possible, for example LBNL's cells operated for 1200 h at 700 °C, Topsoe/DTU cells operated for 3000 h at 650 °C, and Ceres Power cells operated for 6400 h around 600 °C [7,14,15]. Alternatively, cells that are designed for higher-temperature operation could be used, such as plasma-sprayed cells that operate at 750–800 °C [16,17].

4. Summary

Dynamic-temperature operation capability was demonstrated for SOFC cells. A related operation strategy could incorporate rapid temperature variation to match the SOFC power output to a dynamic load requirement. MS-SOFCs are particularly well suited to this application, as they are known to tolerate rapid thermal cycling while not operating. It is demonstrated here that MS-SOFCs can also be operated continuously while the temperature varies; the power density at fixed voltage was shown to more than double in a few minutes. Stack temperature variation may occur on a different timescale, with significant heat available from exothermic reaction counterbalanced by the thermal mass of the stack and other system components. It is anticipated that the dynamic-temperature operation concept demonstrated here may lead to improved SOFC systems with greater operational flexibility, improved efficiency, and reduced cost. Modeling is recommended as a future effort to clarify realistic heating and cooling rates for a stack, identify thermal issues such as heat energy lost from the stack during cooling, and rigorously predict system-level benefits of the dynamic-temperature operation strategy, including efficiency and cost.

Acknowledgements

References

[1] H. Ghezel-Ayagh, B.P. Borglum, Review of progress in solid oxide fuel cells at fuel cell energy, ECS Trans. 78 (2017) 77–86, http://dx.doi.org/10.1149/07801.0077ecst.

[2] R. Leah, A. Bone, E. Hammer, A. Selcuk, M. Rahman, A. Clare, S. Mukerjee, M. Selby, Development progress on the Ceres power steel cell technology platform: further progress towards commercialization, ECS Trans. 78 (2017) 87–95, http://dx.doi.org/10.1149/07801.0087ecst.

[3] A. Mai, F. Fleischhauer, R. Denzler, A. Schuler, Progress in HEXIS' development: galileo 1000 N and HEXIS' next generation SOFC system, ECS Trans. 78 (2017) 97–106, http://dx.doi.org/10.1149/07801.0097ecst.

[4] D. Hickey, M. Alinger, A. Shapiro, K. Brown, T. Striker, H. Wang, S. Gaunt, D. Kinsey, I. Hussaini, Stack development at GE–fuel cells, ECS Trans. 78 (2017) 107–116, http://dx.doi.org/10.1149/07801.0107ecst.

[5] R. Leah, N.P. Brandon, A. Duckett, K.E. Koury, M. Schmidt, Method an Apparatus for Operating a Solid-oxide Fuel Cell Stack with a Mixed Ionic/Electronic Conducting Electrolyte, (2017) US20170301936A1.

[6] M.C. Tucker, A.S. Ying, Metal-supported solid oxide fuel cells operated in direct-flame configuration, Int. J. Hydrogen Energy 42 (2017) 24426–24434, http://dx.doi.org/10.1016/j.ijhydene.2017.07.224.

[7] M.C. Tucker, Durability of symmetric-structured metal-supported solid oxide fuel cells, J. Power Sources 369 (2017) 6–12, http://dx.doi.org/10.1016/j.jpowsour.2017.09.075.

[8] A.M. Dayaghi, K.J. Kim, S.J. Kim, S. Kim, H. Bae, G.M. Choi, Thermal cycling and electrochemical characteristics of solid oxide fuel cell supported on stainless steel with a new 3-phase composite anode, J. Power Sources 354 (2017) 74–84, http://dx.doi.org/10.1016/j.jpowsour.2017.04.022.

[9] L.M. Rodriguez-Martinez, L. Otaegi, M.A. Alvarez, M. Rivas, N. Gomez, A. Zabala, N. Arizmendiarrieta, I. Antepara, A. Urriolabeitia, I. Villarreal, A. Laresgoiti, Degradation studies on tubular metal supported SOFC, ECS Trans. 25 (2009) 745–752.

[10] M.C. Tucker, G.Y. Lau, C.P. Jacobson, L.C. DeJonghe, S.J. Visco, Stability and robustness of metal-supported SOFCs, J. Power Sources 175 (2008) 447–451, http://dx.doi.org/10.1016/j.jpowsour.2007.09.032.

[11] M.C. Tucker, Development of high power density metal-supported solid oxide fuel cells, Energy Technol. 5 (2017) 2175–2181.

[12] M.C. Tucker, G.Y. Lau, C.P. Jacobson, L.C. DeJonghe, S.J. Visco, Performance of metal-supported SOFCs with infiltrated electrodes, J. Power Sources 171 (2007) 477–482, http://dx.doi.org/10.1016/j.jpowsour.2007.06.076.

[13] T.Z. Sholklapper, V. Radmilovic, C.P. Jacobson, S.J. Visco, L.C. De Jonghe, Synthesis and stability of a nanoparticle-infiltrated solid oxide fuel cell electrode, Electrochem. Solid state Lett. 10 (2007) B74–B76, http://dx.doi.org/10.1149/1.2434203.

[14] B.J. McKenna, N. Christiansen, R. Schauperl, P. Prenninger, J. Nielsen, P. Blennow, T. Klemensø, S. Ramousse, A. Kromp, A. Weber, Advances in metal supported cells in the METSOFC EU consortium, Fuel Cell. 13 (2013) 592–597, http://dx.doi.org/10.1002/fuce.201200185.

[15] R. Leah, A. Bone, M. Lankin, A. Selcuk, M. Rahman, A. Clare, L. Rees, S. Phillip, M. Selby, Ceres power steel cell technology: rapid progress towards a truly commercially viable SOFC, ECS Trans. 68 (2015) 95–107.

[16] J. Harris, Y. Yan, R. Bateni, O. Kesler, Degradation of La 0.6 Sr 0.4 Co 0.2 Fe 0.8 O 3- δ -Ce 0.8 Sm 0.2 O 1.9 cathodes on coated and uncoated porous metal supports, Fuel Cell. (2016) 1–11, http://dx.doi.org/10.1002/fuce.201500139.

[17] V.V. Krishnan, Recent developments in metal-supported solid oxide fuel cells, Wiley Interdiscip, Rev. Energy Environ (2017), http://dx.doi.org/10.1002/wene.246 e246.